Supramolecular Inclusion-Based Molecular Integral Rigidity: A Feasible Strategy for Controlling Structural Connectivity of Uranyl Polyrotaxane Networks

*Lei Mei, Lin Wang, Li-yong Yuan, Shu-wen An, Yu-liang Zhao, Zhi-fang Chai, Peter C. Burns and Wei-qun Shi**

Supporting Information

Table of contents

dimensional framework of **1** projected along [100]. (c, without cucurbituril macrocycles; d, with cucurbituril macrocycles). The green sticks in a, b and c indicate the directions of the crystallographic axes, and green rods in d illustrate the channels.

Figure S8. Close packing of 2D uranyl polyrotaxane sheets in compound **1** (a) through widely distributed C-H•••O hydrogen bonding between cucurbituril macrocycles and uranyl motifs (b). Both the cucurbituril macrocycles (c) and uranyl motifs (d) contribute to the hydrogen bonding network by interaction with functional groups of adjacent sheets from two different directions.

Figure S9. 1D regular channels in hydrogen-bonded three-dimensional framework of compound **1** viewed from axis *b* (figure (a) and (b)) or *c* (figure (c)and (d)). Top: without cucurbituril macrocycles; bottom: with cucurbituril macrocycles.

Figure S10. EDS spectrum of CB[6](HCl) revealing the typical peaks of C, N, O and Cl elements.

Figure S11. EDS spectrum of **L1'** revealing the typical peaks of C, N, O and Br elements.

Figure S12. Powder X-Ray diffraction of different products from hydrothermal systems, indicating that introduction of sulphate ion (using uranyl sulphate to repalce uranyl nitrate, or adding sodium sulfate or ammonium sulfate) into the hydrothermal system of uranyl ion and **L1'** affords the same compound (**1)**, which is similar to the system of **L1** and uranyl nitrate.

Figure S13. EDS spectrum of compound **2** revealing the typical peaks of C, N, O, Br and U elements.

Figure S14. Powder X-Ray Diffraction of compound **2**. The upper and lower parts for each diagram are experimental spectra and simulated spectra from single crystal data.

Figure S15. Close packing of 2D uranyl polyrotaxane sheets through widely distributed C-H•••O hydrogen bonding between cucurbituril macrocycles and uranyl motifs for compounds **2** (a). Cationic 2D networks with bromide anions (purple balls) located in the cavities of the networks for **2** (b and c).

Figure S16. Binding experiments of $[C6BPCEt]Br_2$ with $CB[6](H_2SO_4)$ in D_2O-HCOOH (1:1, v/v). Concentrations: a) $[C6BPCEt]Br_2$; b) $CB[6](H_2SO_4)/[C6BPCEt]Br_2$ = 0.052/0.011 mol/L; c) $CB[6](H_2SO_4)$ /$[C6BPCEt]Br_2$ = 0.010/0.011 mol/L; d) L1.

Figure S17. Binding experiments of $[C6BPCEt]Br_2$ with CB[6](HCl) in D_2O-HCOOH (1:1, v/v). Concentrations: a) $[C6BPCEt]Br_2$; b) CB[6](HCl) /$[C6BPCEt]Br_2$ = 0.0067/0.012 mol/L; c) CB[6](HCl) /$[C6BPCEt]Br_2$ = 0.011/0.011 mol/L; d) L1'.

Figure S18. Binding experiments of $[C6BPCEt]Br_2$ with CB[7](HCl) in pure D_2O and in D_2O-HCOOH (1:1, v/v). Concentrations: a) $[C6BPCEt]Br_2$; b) CB[7](HCl) /$[C6BPCEt]Br_2$ = 0.0061/0.011 mol/L in pure D_2O; c) CB[7](HCl) /$[C6BPCEt]Br_2$ = 0.012/0.011 mol/L in pure D_2O; d) CB[7](HCl) /$[C6BPCEt]Br_2$ = 0.0055/0.0097 mol/L D_2O-HCOOH (1:1, v/v); e) CB[7](HCl) /$[C6BPCEt]Br_2$ = 0.0099/0.011 mol/L in D_2O-HCOOH (1:1, v/v); f) L2.

Figure S19. EDS spectrum of CB[7](HCl) revealing the typical peaks of C, N, O and Cl elements.

Figure S20. EDS spectrum of **L2** revealing the typical peaks of C, N, O and Br elements.

Figure S21. EDS spectrum of compound **3** revealing the typical peaks of C, N, O, Br and U elements.

Figure S22. Powder X-Ray Diffraction of compound **3**. The upper and lower parts for each diagram are experimental spectra and simulated spectra from single crystal data.

Figure S23. Structural building unit of compounds **3** containing a uranyl center in **s**even-fold coordination pentagonal biyramid geometry and rotaxane linkers with folded string chains.

Figure S24. C-H•••O hydrogen bonding between cucurbituril macrocycles and uranyl motifs in

S3. Tables

S1. Synthesis and characterization for some compounds

General Methods.

Caution! Suitable measures for precautions and protection should be taken, and all operations should follow the criteria while handling such substances although natural uranium was used in the experiment. All the reagents were purchased from commercial sources and used as received. CB[6](H_2SO_4) was synthesized from glycoluril and formaldehyde aqueous solution (40%) in concentrated H_2SO_4 and CB[6](HCl) and CB[7](HCl) was synthesized from glycoluril and paraformaldehyde in HCl aqueous solution according to the reported procedure.[1]

^{1}H-NMR spectra were recorded on a Bruker AVANCE III (500 MHz, Bruker, Switzerland) with deuterium oxide (D2O) or D2O-formic acid (1:1, v/v) as a solvent. ESI-MS spectra were obtained with a Bruker AmaZon SL ion trap mass spectrometer (Bruker, USA). The energy dispersive x-ray spectroscopy (EDS) of crystals for elemental analysis was performed with SEM (S-4800, HITACHI) at an accelerating voltage of 1.0 kV. Powder XRD measurements (PXRD) were recorded on a Bruker D8 Advance diffractometer with Cu Kα radiation (λ=1.5406 Å) in the range 5-80°(step size: 0.02º). Thermogravimetric analysis (TGA) was performed on a TA Q500 analyzer over the temperature range of 25-800 °C in air atmosphere with a heating rate of 5 °C/min. The Fourier transform infrared (IR) spectra were recorded from KBr pellets in the range of 4000-400 cm^{-1} on at Bruker Tensor 27 spectrometer. Solid-state fluorescence spectra were measured on a Hitachi F-4600 fluorescence spectrophotometer.

Synthesis.

1,1'-(hexane-1,6-diyl)bis(4-(ethoxycarbonyl)pyridine-1-ium) bromide ([C6BPCEt]Br_2). [C6BPCEt]Br_2 was synthesized according to the reported procedure.[2-3] A mixture of 1,6-dibromohexane (4.88 g, 20 mmol) and isonicotinate (6.40 g, 40 mmol) dissolved in 150 ml of acetonitrile was refluxed for 48 h. After cooling to room temperature, the solution was concentrated to ~30 ml by evaporation in vacuum and a yellow solid was obtained. The crude residues were filtered, washed with acetone, and dried under vacuum to afford the final product, [C6BPCEt]Br_2. Yield: 4.95 g (43.9%). ^{1}H NMR (500MHz, D_2O, δ ppm): 8.99 (d, 4H); 8.46 (d, 4H), 4.63 (t, 4H), 4.44 (t, 4H), 1.99 (m, 4H), 1.36 (m, 4H), 1.34 (m, 6H). MS (ESI): mass calculated for $C_{22}H_{30}N_2O4^{2+}$ (M^{2+}), 386.22; m/z found, 192.96 (M^{2+}/2).

Scheme S1. Synthesis of pseudorataxane precursors **L1**, **L1'** and **L2**, and uranyl compounds **1-3**. The barrel-like cartoons in the molecular structure represent simplified depiction of cucurbit[6]uril (CB[6]) and cucurbit[7]uril (CB[7]).

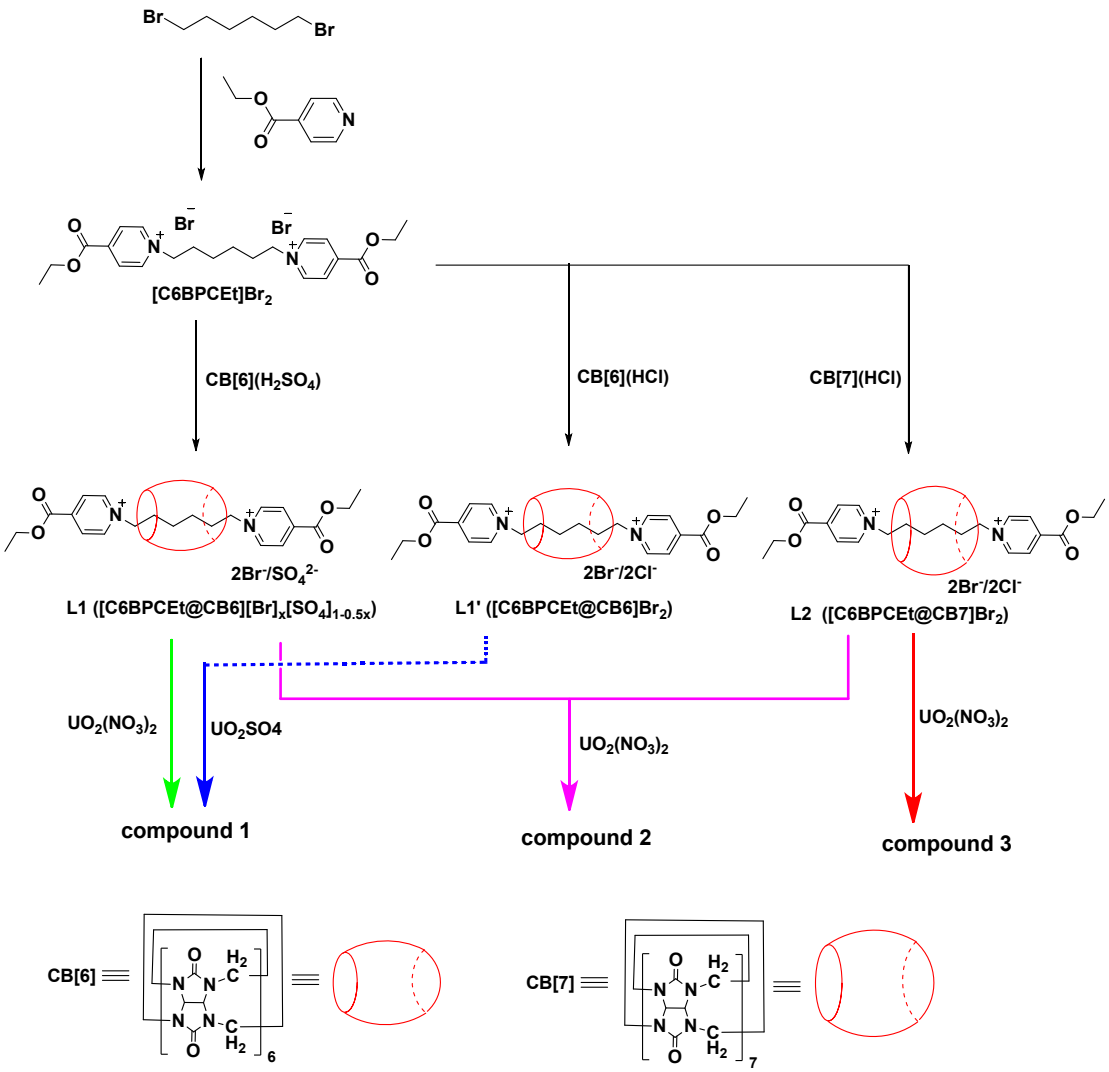

Scheme S2. Synthesis of $[C6BPCA][Cl]_2$ and $[C6BPCA@CB6][Cl]_x[SO4]_{1-x}$.

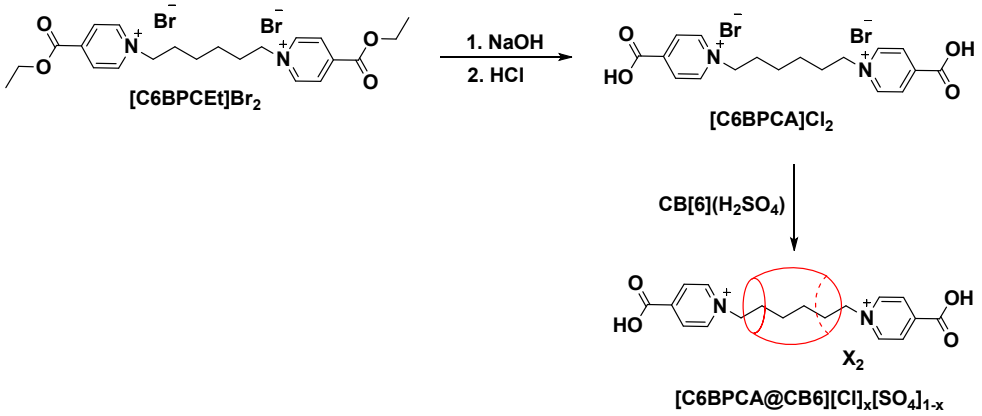

Scheme S3. Synthesis of the hydrolysis products of **L1** in two forms, **[C6BPCA@CB6][NO_3]$_2$** and **C6BPC@CB6**.

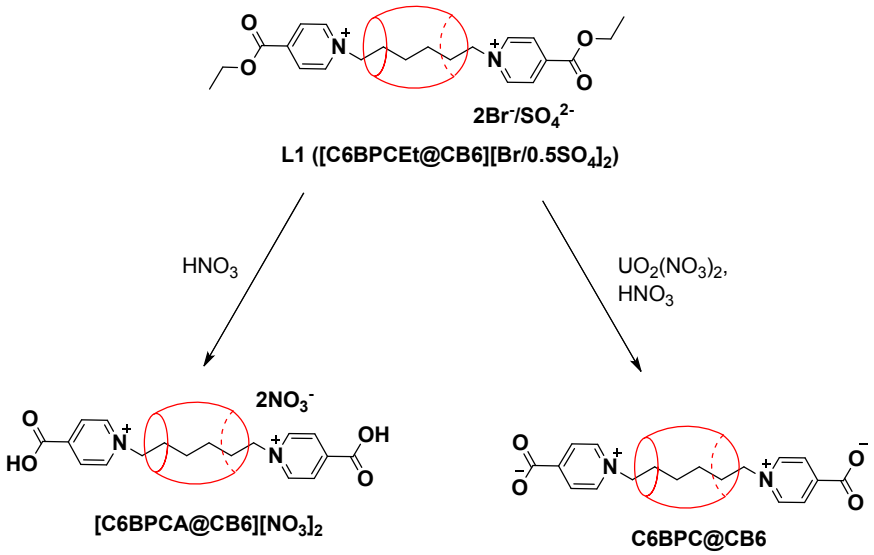

The pseudorotaxane precursors, **L1, L1' and L2,** were synthesized according to the procedures reported previously.[4]

L1 ([C6BPCEt@CB6][Br]$_x$[SO_4]$_{1-x}$). ^{1}H NMR (500MHz, D_2O, δ ppm): 9.50 and 9.47 (d and d, 4H); 8.41 and 8.34 (d and d, 4H), 5.65 (d, 12H), 5.45 (s, 12H), 4.44 (m, 8H), 4.21 (d, 12H), 1.35 (t, 6H), 1.13 (m, 4H), 0.50 (m, 4H). MS (ESI): mass calculated for $C_{58}H_{66}N_{26}O_{16}^{2+}$ (M^{2+}), 1382.51; m/z found, 691.21 (M^{2+}/2).

L1' ([C6BPCEt@CB6]Br_2). ^{1}H NMR (500MHz, D_2O, δ ppm): 9.50 and 9.41 (d and d, 4H); 8.41 and 8.24 (d and d, 4H), 5.64 (dd, 12H), 5.45 (s, 12H), 4.44 (m, 8H), 4.21 (d, 12H), 1.35 (t, 6H), 1.13 (m, 4H), 0.50 (m, 4H). MS (ESI): mass calculated for $C_{58}H_{66}N_{26}O_{16}^{2+}$ (M^{2+}), 1382.51; m/z found, 691.29 (M^{2+}/2).

L2 ([C6BPCEt@CB7]Br_2). ^{1}H NMR (500MHz, D_2O, δ ppm): 8.86 and 8.82 (d and m, 4H); 8.59 and 8.43 (d and m, 4H), 5.65 (dd, 12H), 5.47 (s, 12H), 4.48 (q, 4H), 4.17 (d, 12H), 3.90 (m, 4H), 1.37 (t, 6H), 1.27 (m, 4H), 0.65 (m, 4H). MS (ESI): mass calculated for $C_{64}H_{72}N_{30}O_{18}^{2+}$ (M^{2+}), 1548.56; m/z found, 774.17 (M^{2+}/2).

[C6BPCA]Cl_2. [C6BPCEt]Br_2 were synthesized according to the procedures reported previously[2, 3]. [C6BPCEt]Br_2 (1.00 g, 1.8 mmol) was dissolved in 20 ml of NaOH (1M) and the mixture was heated at 60 °C for 4 h. After cooling to room temperature, the solution was concentrated to ~5 ml by evaporation in vacuum and the solution pH was adjusted to 1~2 by adding a solution of HCl (6M). The obtained crude precipitates were filtered, washed with water and acetone, and dried under vacuum to afford the final product, **[C6BPCA]Cl_2**. ^{1}H NMR

(500MHz, D_2O, δ ppm): 8.89 (d, 4H); 8.34 (d, 4H), 4.58 (t, 4H), 4.44 (t, 4H), 1.95 (m, 4H), 1.33 (m, 4H). MS (ESI): mass calculated for $C_{18}H_{22}N_2O4^{2+}$ (M^{2+}), 330.16; m/z found, 164.95 (M^{2+}/2).

[C6BPCA@CB6][Cl]$_x$[SO4]$_{1-x}$. The pseudorotaxane precursor [C6BPCA@CB6][Cl]$_x$[SO4]$_{1-x}$ were synthesized according to the procedures reported previously.[4] ^{1}H NMR (500MHz, D_2O, δ ppm): 9.35 and 9.34 (d and d, 4H); 8.34 and 8.16 (d and d, 4H), 5.61 (d, 12H), 5.45 (s, 12H), 4.49 (m, 4H), 4.16 (d, 12H), 1.01 (m, 4H), 0.48 (m, 4H). MS (ESI): mass calculated for $C_{54}H_{58}N_{26}O_{16}^{2+}$ (M^{2+}), 1326.45; m/z found, 663.06 (M^{2+}/2).

The carboxylic acid forms of L1 ([C6BPCA@CB6][NO$_3$]$_2$). The pseudorotaxane precusor **L1** (0.040 g) was dissolved in water (1 mL) and sealed in a stainless-steel bomb at 150°C for 48 h. When being cooled to room temperature, colorless block crystals were formed. The obtained colorless block crystals were washed with water and dried in air to afford **[C6BPCA@CB6][NO$_3$]$_2$**.

[C6BPC@CB6]. $UO_2(NO_3)_2·6H_2O$ (70 μL, 0.035 mmol) were added to a suspension of the pseudorotaxane ligand of **L1** (0.052 g, 0.070 mmol) in water (1 mL) in a stainless-steel bomb. The reaction mixture was treated with 10 μL of HNO_3 , and then was sealed, kept at 150°C for 48 h. After gradually cooling to room temperature, yellow prismatic crystals of compound **1** as well as a small amount of colorless block crystals (corresponding to another hydrolysis product of **L1**, **[C6BPC@CB6]** in the zwitter-ion form) were obtained.

1: $UO_2(NO_3)_2·6H_2O$ (70 μL, 0.035 mmol) were added to a suspension of the pseudorotaxane ligand of **L1** (0.052 g, 0.070 mmol) in water (1 mL) in a stainless-steel bomb. The mixture was sealed, kept at 150°C for 48 h and gradually cooled to room temperature. The obtained yellow prismatic crystals were washed with water and ethanol and dried in air to afford compound 1. Starting from other reaction agents including: (1) UO_2SO_4 (70 μL, 0.035 mmol) and **L1'** (0.054g, 0.070 mmol); $UO_2(NO_3)_2·6H_2O$ (70 μL, 0.035 mmol), $(NH_4)_2SO4$ (12 mg) and **L1'** (0.054g, 0.070 mmol), and (3) $UO_2(NO_3)_2·6H_2O$ (70 μL, 0.035 mmol), Na_2SO4 (10 mg) and **L1'** (0.052 g, 0.070 mmol) also afford a phase-pure compound **1**.

2 and **3**: Compound **2** was prepared through a similar procedure from the combination of ligands of **L1** and **L2**. Compound **3** were prepared through a similar procedure from the ligands of **L2**.

X-ray Single Structural Determination.

X-ray diffraction data for compounds **C6BPC@CB6**, **[C6BPCA@CB6][NO$_3$]$_2$**, **1** and **2** were collected on Agilent SuperNova X-ray CCD diffractometer with a Cu Kα (λ = 1.54184 Å) or Mo Kα (λ = 0.71073 Å) X-ray source at room temperature or 150 K according to the nature of crystal sample. Standard Agilent Crysalis software was used for determination of the unit cells and data collection control. The crystal structures were solved by means of direct methods and refined with

full-matrix least squares on SHELXL-97. Data collection of the compound **3** was performed with synchrotron radiation facility at BSRF (beamline 3W1A of Beijing Synchrotron Radiation Facility, λ = 0.71073 Å) using a MAR CCD detector. The crystal was mounted in nylon loops and cooled in a cold nitrogen-gas stream at 100 K. Data were indexed, integrated and scaled using DENZO and SCALEPACK from the HKL program suite. The crystal structures were solved by means of direct methods and refined with full-matrix least squares on SHELXL-97. In compounds **1**-**3**, the unit cell includes a large region of disordered solvent water molecules, which could not be modeled as discrete atomic sites. We employed PLATON/SQUEEZE to produce a set of solvent-free diffraction intensities, which is used to make a further refinement. Crystallographic data for the structures in this paper have been deposited with the Cambridge Crystallographic Data Centre as supplementary publication nos. CCDC-1058135 (**C6BPC@CB6**), CCDC-1058136 (**[C6BPCA@CB6][NO_3]$_2$**), CCDC-1058137 (**1**), CCDC-1058139 (**2**) and CCDC-1058140 (**3**).

Crystal data for **C6BPC@CB6 (**CCDC-1058135**)**: $C_{54}H_{56}N_{26}O_{16}$, $C_{18}H_{20}N_2O_4$@CB6, Mr = 1325.25, triclinic, $P\bar{1}$, *a* = 12.0755(7) Å, *b* = 12.3189(6) Å, *c* = 12.3197(6) Å, alpha = 106.538(4)°, beta = 97.085(5)°, gamma= 107.693(5)°, V = 1628.92(15) Å^3, Z = 1, $\rho_{calcd.}$= 1.351 g•cm^{-3}. Of the 11534 reflections collected, 5822 were unique (R_{int} = 0.0190). Refinement on all data converged at R_1 = 0.0492 and wR_2 = 0.1225, and GOF = 1.055 for4872 reflections [I > 2σ(I)].

Crystal data for **[C6BPCA@CB6][NO_3]$_2$** (CCDC-1058136): $C_{108}H_{104}N_{56}O_{44}$, $[(C_{18}H_{22}N_2O_4$@CB6)$(NO_3)_2]_2$, Mr = 2890.47, triclinic, $P\bar{1}$, *a* = 12.5869(4) Å, *b* = 16.1378(8) Å, *c* = 16.7184(6) 17.8631(7) Å, alpha= 87.780(4)°, beta= 89.749(3)°, gamma= 67.888(4)°, V = 3358.8(2) Å^3, Z = 1, $\rho_{calcd.}$= 1.429 g•cm^{-3}. Of the 19476 reflections collected, 11508 were unique (R_{int} = 0.0730). Refinement on all data converged at R_1 = 0.2422 and wR_2 = 0.5971, and GOF = 2.191 for 6002 reflections [I > 2σ(I)].

Crystal data for **1 (**CCDC-1058137**)**: $C_{54}H_{56}N_{26}O_{22}SU$, $UO_2(C_{18}H_{20}N_2O_4$@CB6)(SO_4), Mr = 1691.34, triclinic, $P\bar{1}$, *a* = 15.4905(4) Å, *b* = 15.7934(5) Å, *c* = 16.7184(6) Å, alpha= 68.423(3)°, beta= 89.602(3)°, gamma= 83.048(3)°, V = 3772.4(2) Å^3, Z = 2, $\rho_{calcd.}$= 1.489 g•cm^{-3}. Of the 27126 reflections collected, 13434 were unique (R_{int} = 0.0318). Refinement on all data converged at R_1 = 0.0354 and wR_2 = 0.0985, and GOF = 1.057 for12397 reflections [I > 2σ(I)].

Crystal data for **2 (**CCDC-1058139**)**: $C_{108}H_{112}Br_2N_{52}O_{34}U$, $UO_2(C_{18}H_{20}N_2O_4$@CB6$)_2Br_2$, Mr = 3080.35, triclinic, $P\bar{1}$, *a* = 12.6458(3) Å, *b* = 15.6109(3) Å, *c* = 17.1344(5) Å, alpha= 89.597(2)°, beta= 82.238(2)°, gamma= 84.826 (2)°, V = 3282.6(2) Å^3, Z = 1, $\rho_{calcd.}$= 1.532 g•cm^{-3}. Of the 23885 reflections collected, 11910 were unique (R_{int} = 0.0240). Refinement on all data converged at R_1 = 0.0484 and wR_2 = 0.1329, and GOF = 1.045 for 11909 reflections [I > 2σ(I)]. One of the carboxylate groups are disordered showing two possible coordination modes, with η^1-mode and η^2-mode coordination were given occupancy factors of 0.5 each.

Crystal data for **3 (**CCDC-1058140**)**: $C_{120}H_{136}Br_2N_{60}O_{46}U_2$, $[UO_2(H_2O)_3(C_{18}H_{20}N_2O_4$@CB7$)]_2Br_2$, Mr = 3790.77, triclinic, $P\bar{1}$, *a* =13.333(3) Å, *b* = 26.409(5)

Å, *c* = 26.515(5) Å, alpha= 81.73(3)°, beta= 84.73(3)°, gamma= 84.24(3)°, V = 9164(3) $Å^3$, Z = 2, $\rho_{calcd.}$= 1.374 g•cm^{-3}. Of the 18846 reflections collected, 18846 were unique (R_{int} = 0.077). A full set of data was collected, however the very high angle data was dominated by noise [I < σ(I)] and was omitted. This is primarily due to weak diffraction of macromolecular structures. Refinement on all data converged at R_1 = 0.0726 and wR_2 = 0.1960, and GOF = 1.038 for 16156 reflections [I > 2σ(I)].

Reference

1. Day, A.; Arnold, A. P.; Blanch, R. J.; Snushall, B. *J. Org. Chem.*, **2001**, 66, 8094-8100.
2. Huang, F.H.; Slebodnick, C.; Mahan, E.J.; Gibson, H.W. *Tetrahedron*, **2007**, *63*, 2875-2881.
3. Sun, X. Z.; Li, B.; Xia, C. L.; Zhou, X. H.; Zhang, H.B. *CrystEngComm*, **2012**, *14*, 8525-8529.
4. Mei, L.; Wu, Q. Y.; Liu, C. M.; Zhao, Y. L.; Chai, Z. F.; Shi, W. Q., *Chem. Commun.* **2014,** *50*, 3612-3615.

S2. Typical figures

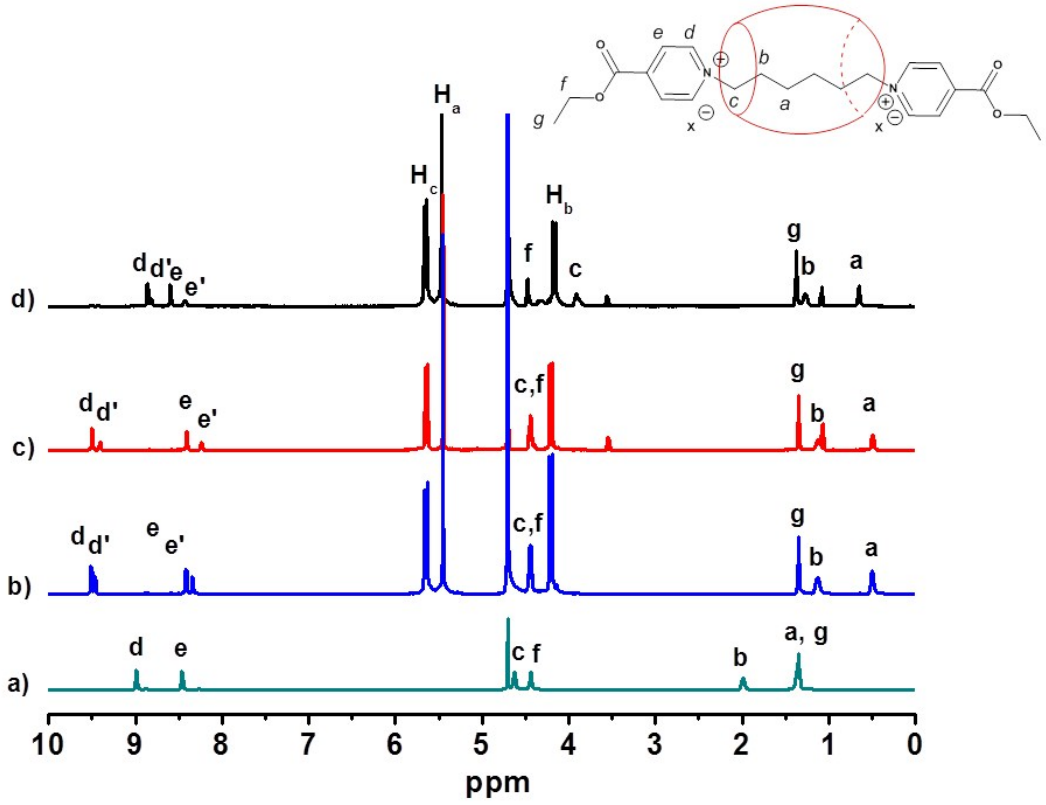

Figure S1. Partial ^{1}H NMR spectra (500 MHz, 298 K, D_2O) of a) **L2**, b) **L1'**, c) **L1**, and d) the axle molecule $[C6BPCEt]Br_2$.

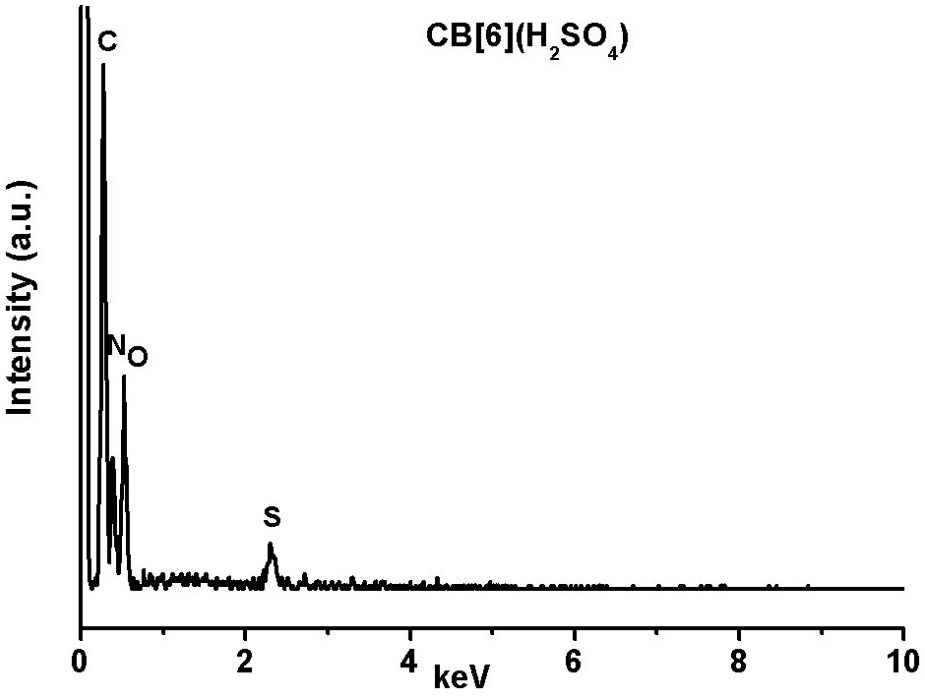

Figure S2. EDS spectrum of $CB[6](H_2SO_4)$ revealing the typical peak of S element.

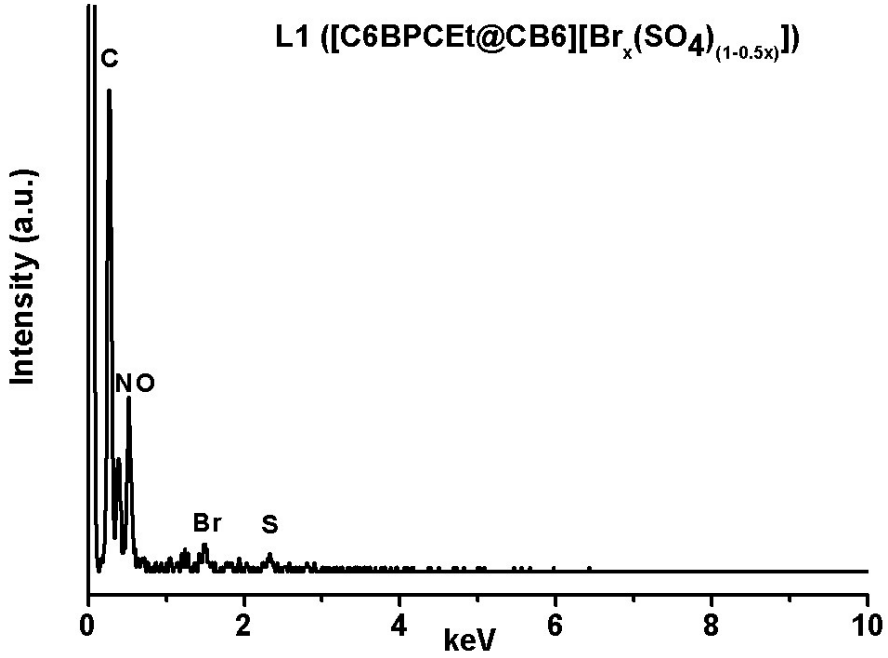

Figure S3. EDS spectrum of **L1** revealing the typical peaks of C, N, O, Br and S elements.

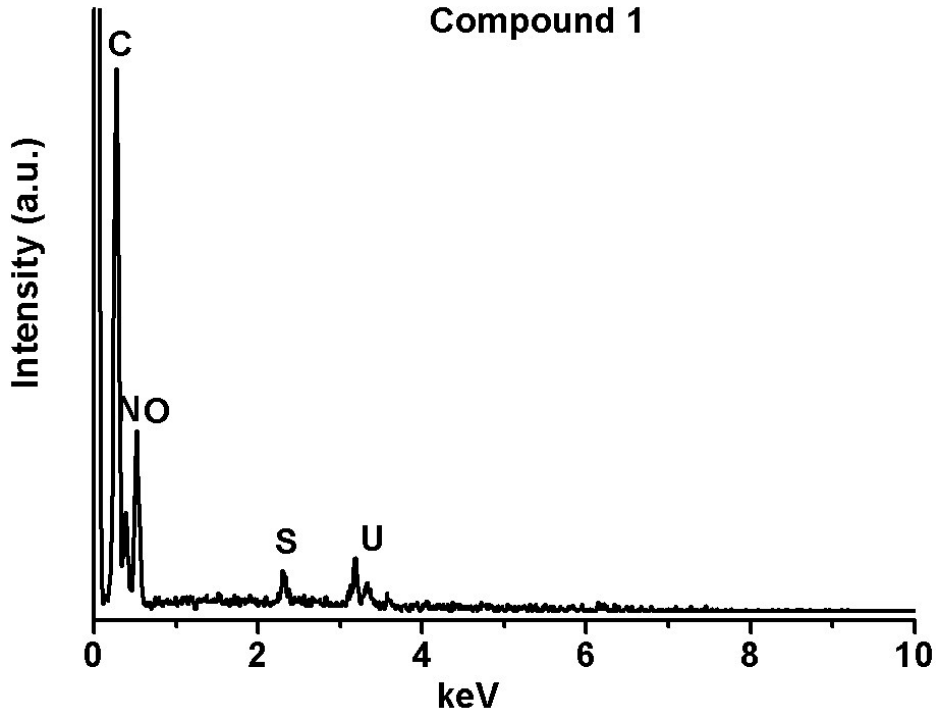

Figure S4. EDS spectrum of compound **1** revealing the typical peaks of C, N, O, S and U elements.

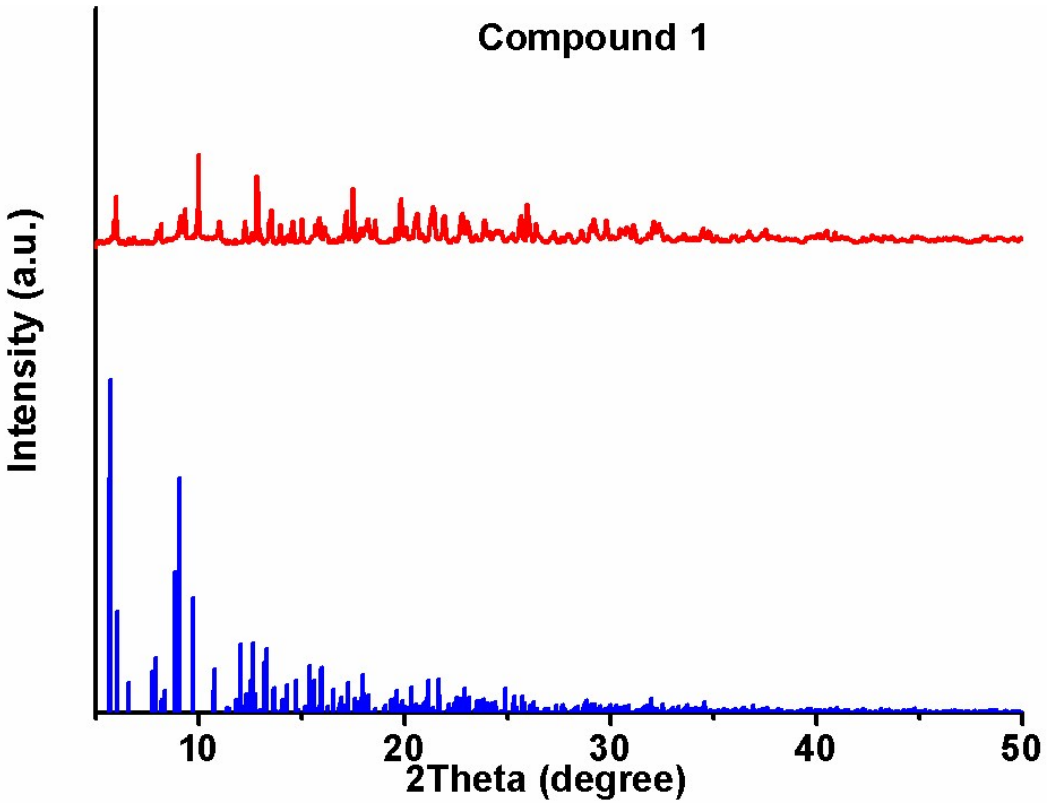

Figure S5. Powder X-Ray Diffraction of compound **1**. The upper and lower parts for each diagram are experimental spectra and simulated spectra from single crystal data.

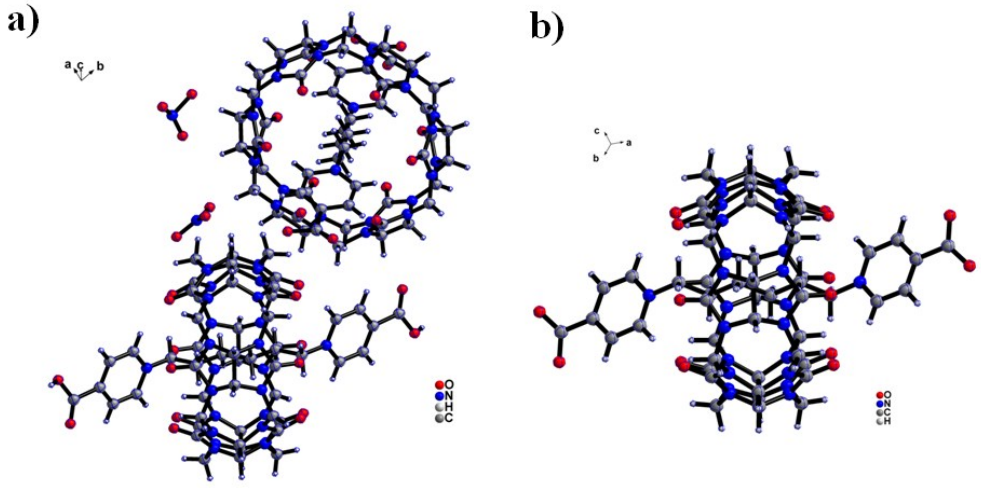

Figure S6. Crystal structures of the hydrolysis products of **L1, [C6BPCA@CB6][NO_3]$_2$ and C6BPC@CB6**.

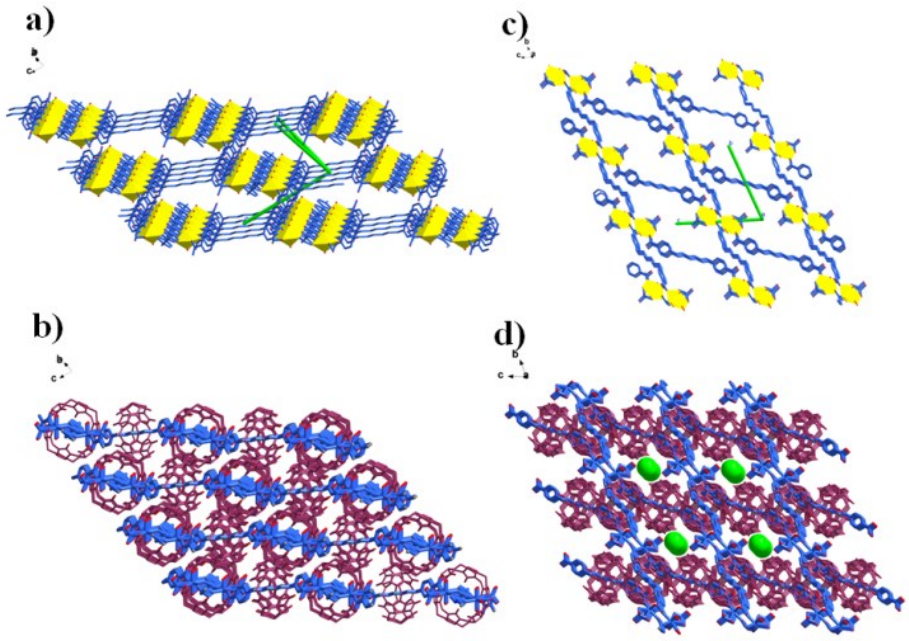

Figure S7. (a-b): A hydrogen-bonded three-dimensional framework of **1** constructed through widely distributed C-H•••O hydrogen bonding between cucurbituril macrocycles and uranyl motifs from two adjacent 2D uranyl polyrotaxane sheets (a, without cucurbituril macrocycles; b, with cucurbituril macrocycles). (c-d): 1D regular channels the in hydrogen-bonded three-dimensional framework of **1** projected along [100]. (c, without cucurbituril macrocycles; d, with cucurbituril macrocycles). The green sticks in a, b and c indicate the directions of the crystallographic axes, and green rods in d illustrate the channels.

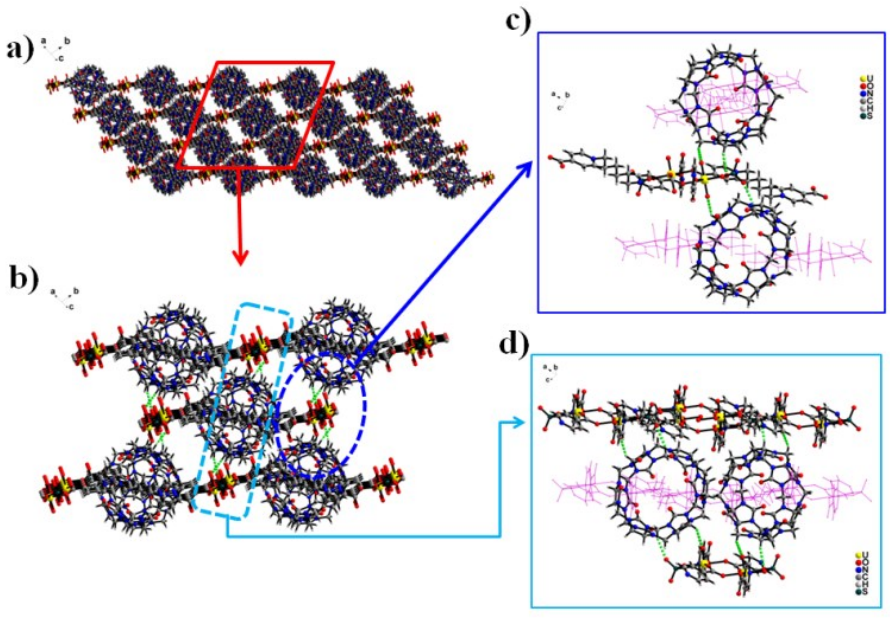

Figure S8. Close packing of 2D uranyl polyrotaxane sheets in compound **1** (a) through widely distributed C-H•••O hydrogen bonding between cucurbituril macrocycles and uranyl motifs (b). Both the cucurbituril macrocycles (c) and uranyl motifs (d) contribute to the hydrogen bonding network by interaction with functional groups of adjacent sheets from two different directions.

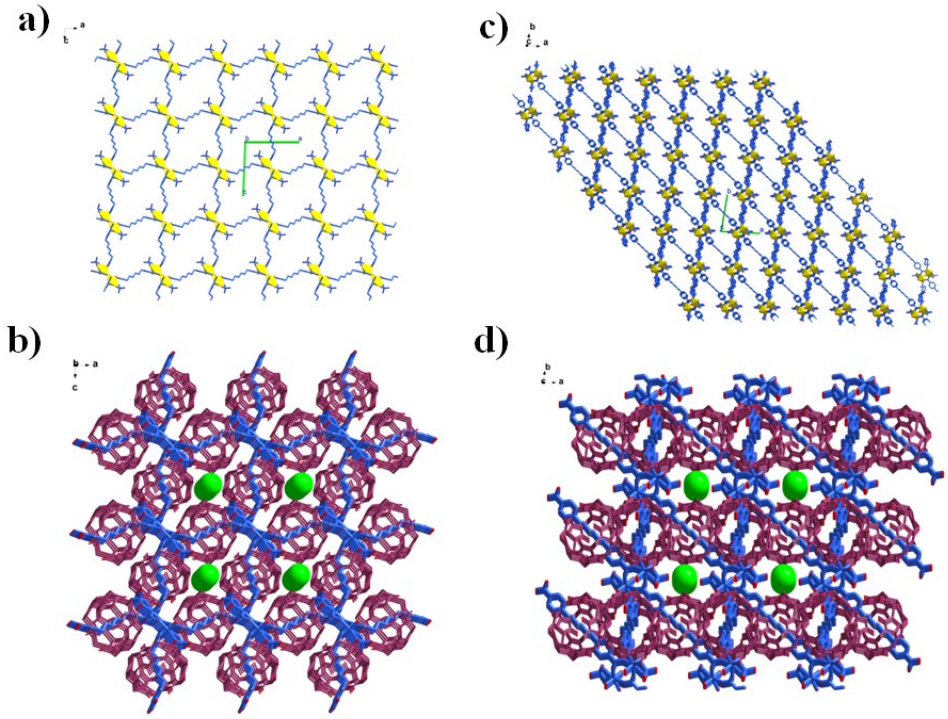

Figure S9. 1D regular channels in hydrogen-bonded three-dimensional framework of compound **1** viewed from axis *b* (figure (a) and (b)) or *c* (figure (c)and (d)). Top: without cucurbituril macrocycles; bottom: with cucurbituril macrocycles.

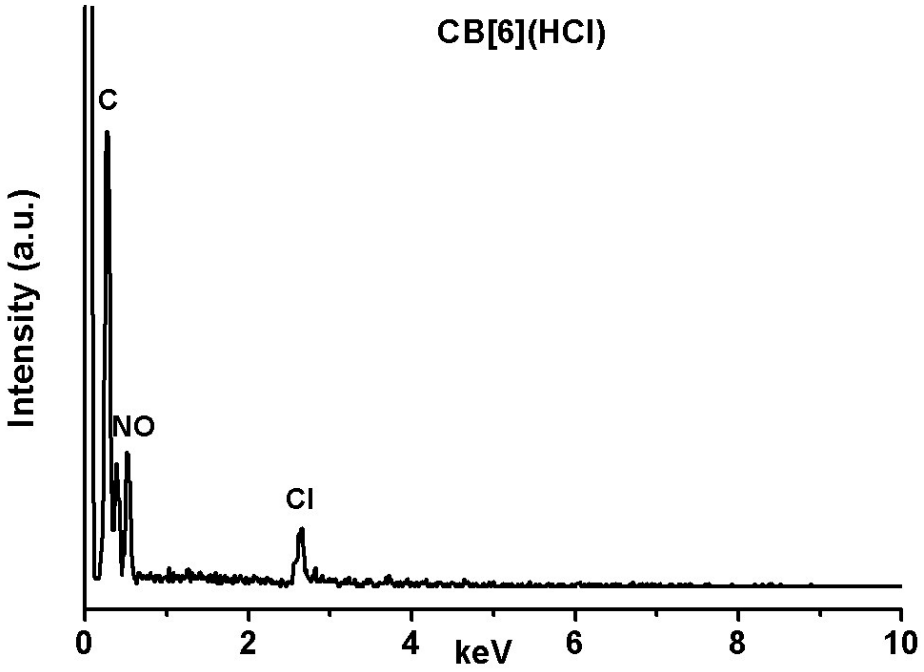

Figure S10. EDS spectrum of CB[6](HCl) revealing the typical peaks of C, N, O and Cl elements.

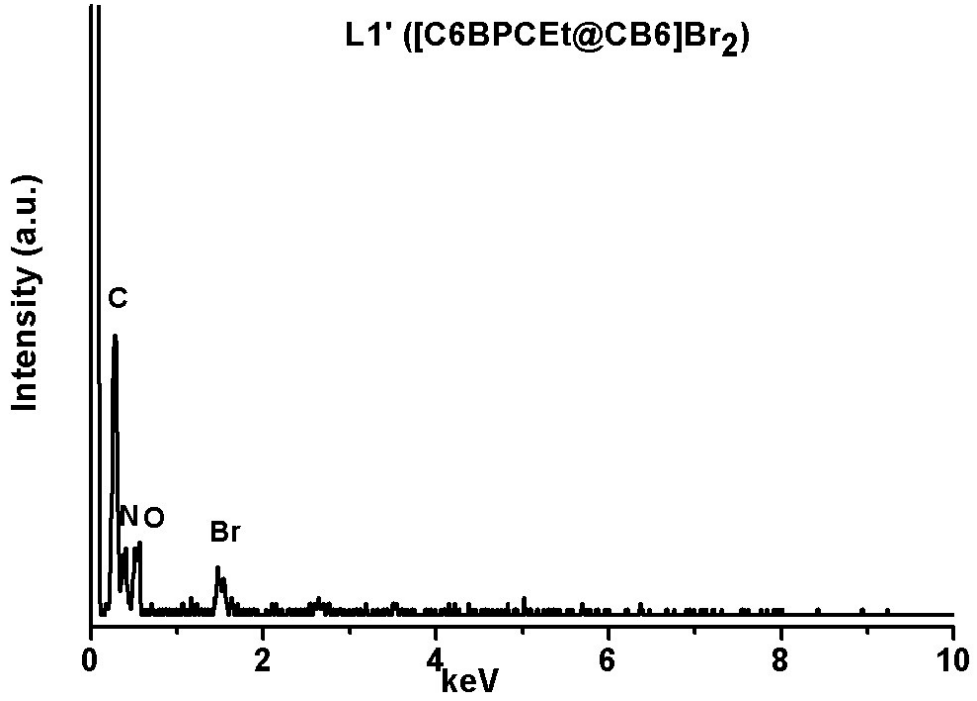

Figure S11. EDS spectrum of **L1'** revealing the typical peaks of C, N, O and Br elements.

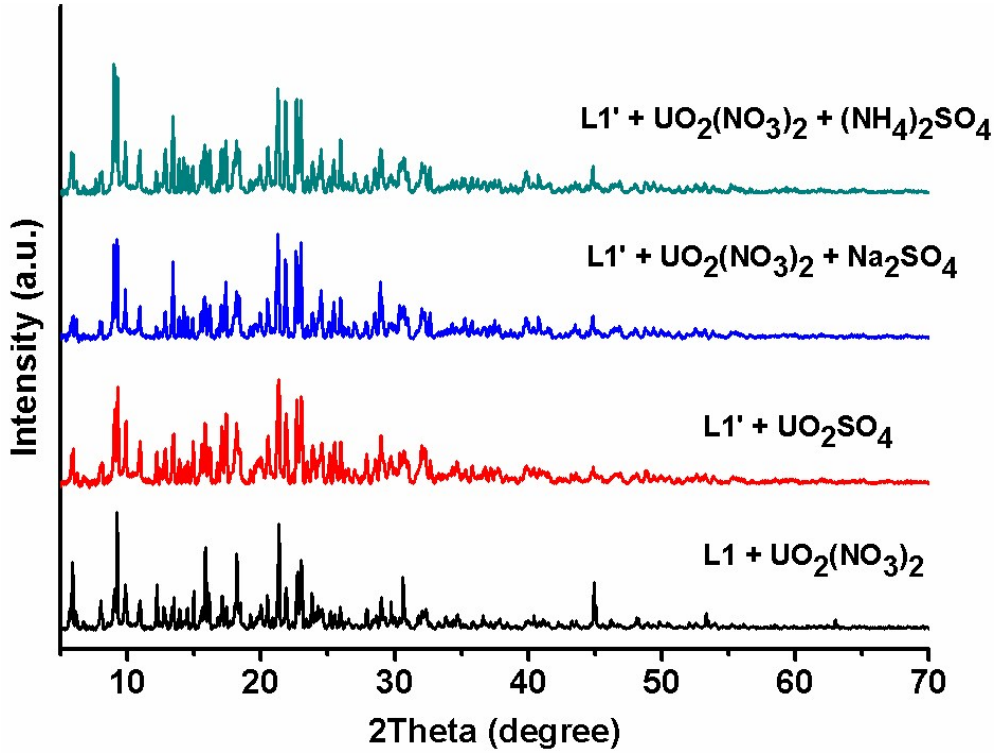

Figure S12. Powder X-Ray diffraction of different products from hydrothermal systems, indicating that introduction of sulphate ion (using uranyl sulphate to repalce uranyl nitrate, or adding sodium sulfate or ammonium sulfate) into the hydrothermal system of uranyl ion and **L1'** affords the same compound (**1**), which is similar to the system of **L1** and uranyl nitrate.

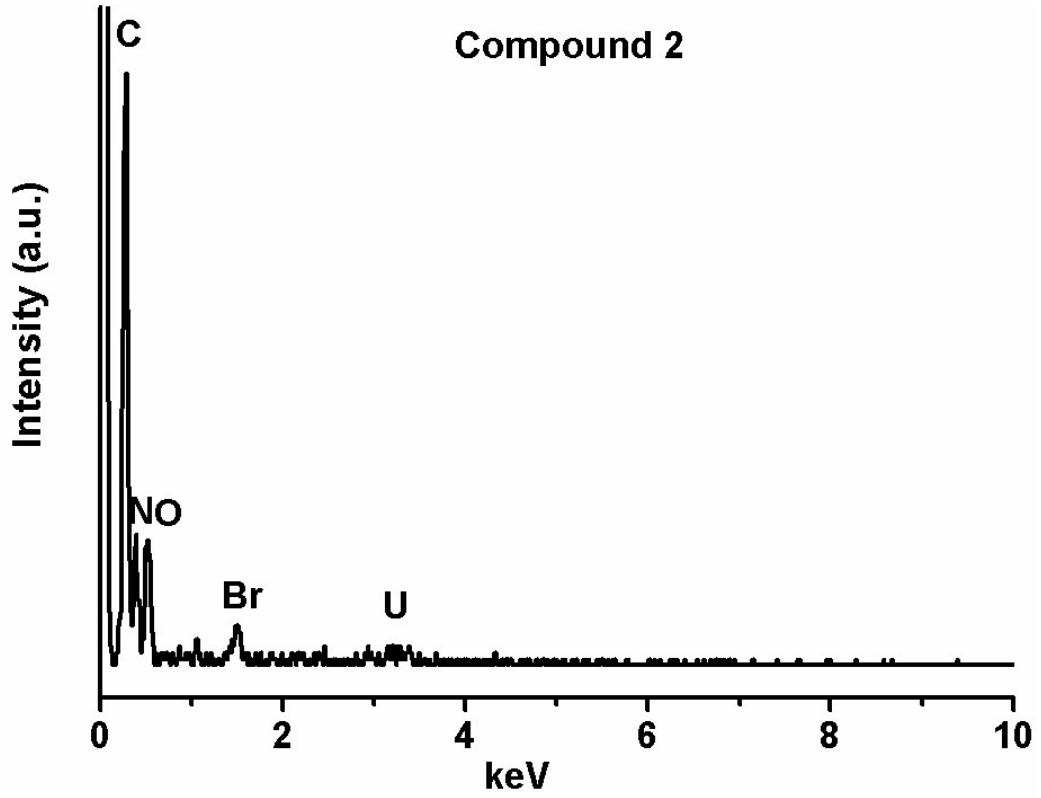

Figure S13. EDS spectrum of compound **2** revealing the typical peaks of C, N, O, Br and U elements.

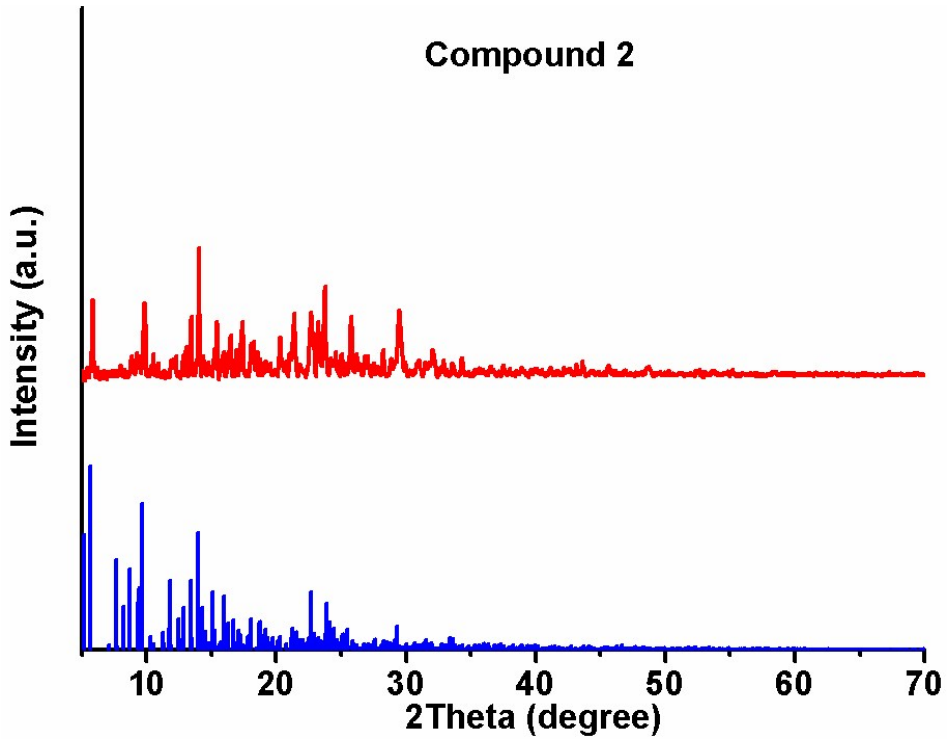

Figure S14. Powder X-Ray Diffraction of compound **2**. The upper and lower parts for each diagram are experimental spectra and simulated spectra from single crystal data.

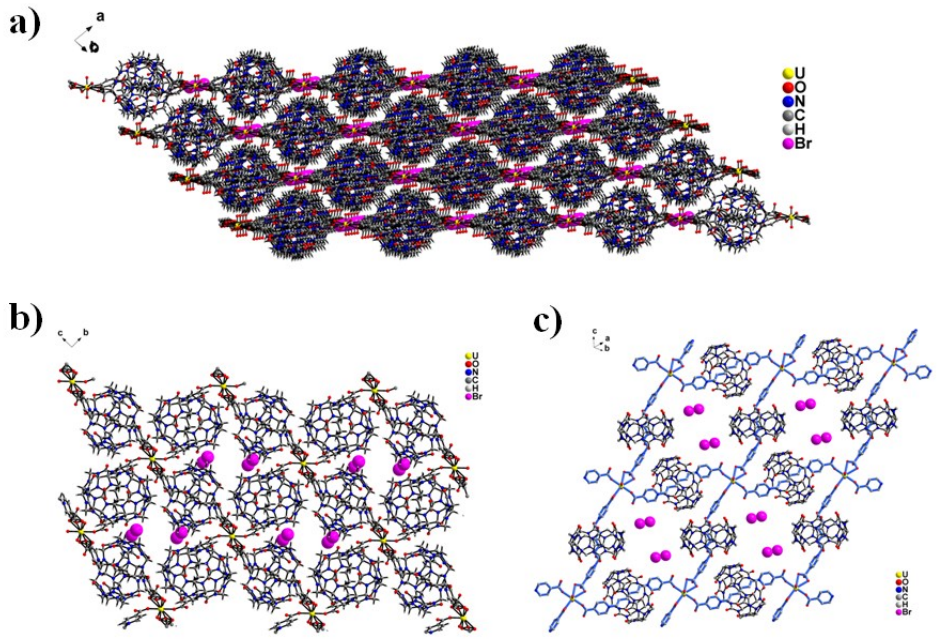

Figure S15. Close packing of 2D uranyl polyrotaxane sheets through widely distributed C-H•••O hydrogen bonding between cucurbituril macrocycles and uranyl motifs for compounds **2** (a). Cationic 2D networks with bromide anions (purple balls) located in the cavities of the networks for **2** (b and c).

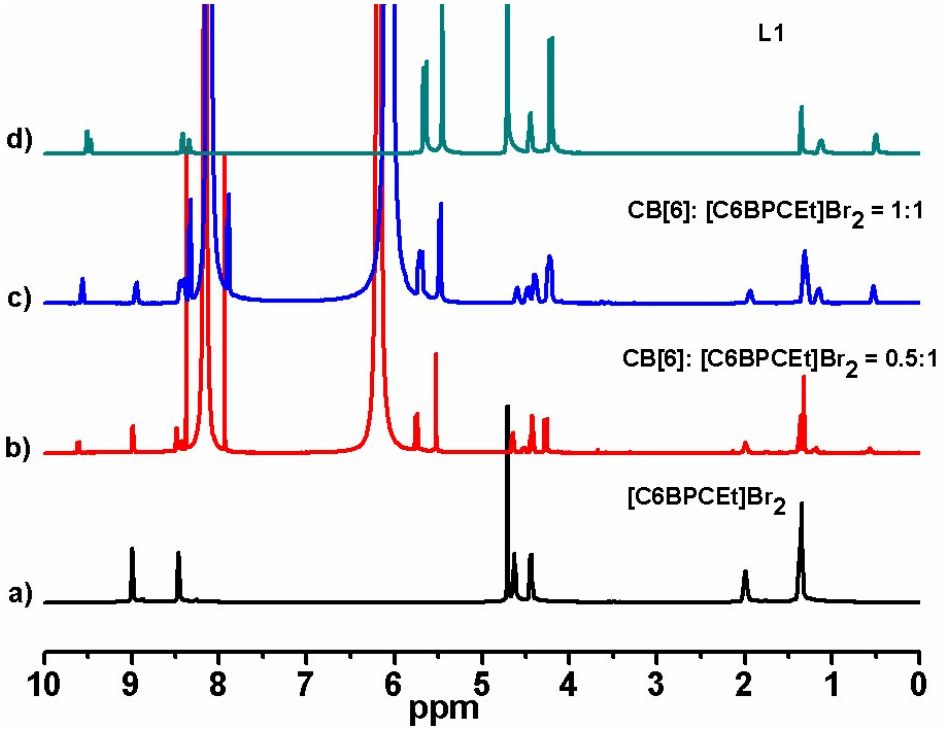

Figure S16. Binding experiments of $[C6BPCEt]Br_2$ with $CB[6](H_2SO_4)$ in D_2O-HCOOH (1:1, v/v). Concentrations: a) $[C6BPCEt]Br_2$; b) $CB[6](H_2SO_4)/[C6BPCEt]Br_2$ = 0.052/0.011 mol/L; c) $CB[6](H_2SO_4)$ /$[C6BPCEt]Br_2$ = 0.010/0.011 mol/L; d) L1.

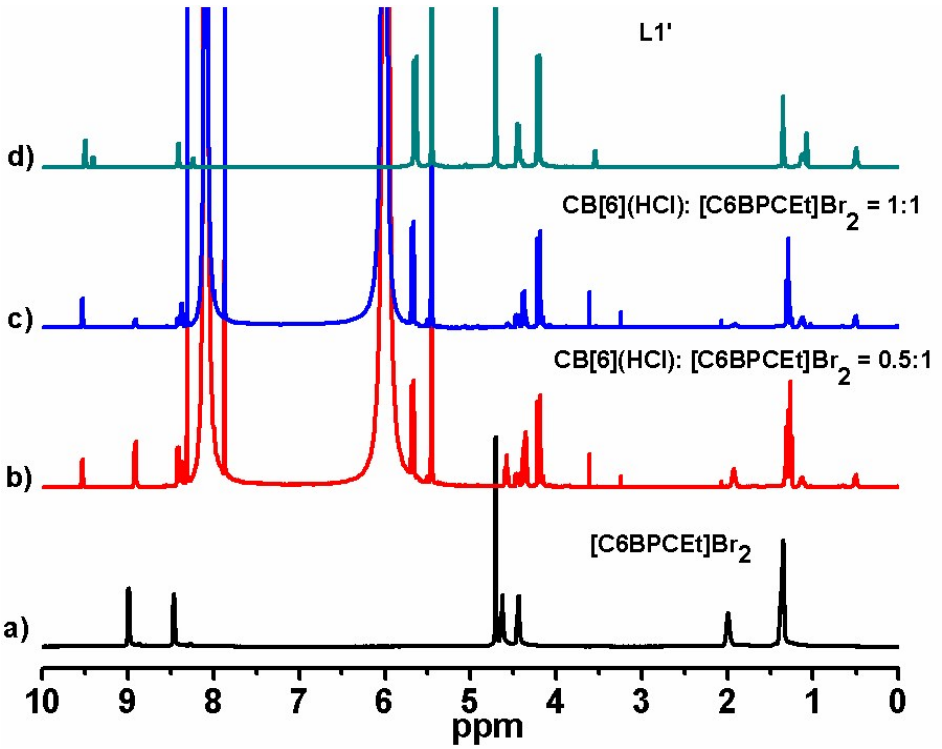

Figure S17. Binding experiments of $[C6BPCEt]Br_2$ with CB[6](HCl) in D_2O-HCOOH (1:1, v/v). Concentrations: a) $[C6BPCEt]Br_2$; b) CB[6](HCl) /$[C6BPCEt]Br_2$ = 0.0067/0.012 mol/L; c) CB[6](HCl) /$[C6BPCEt]Br_2$ = 0.011/0.011 mol/L; d) L1'.

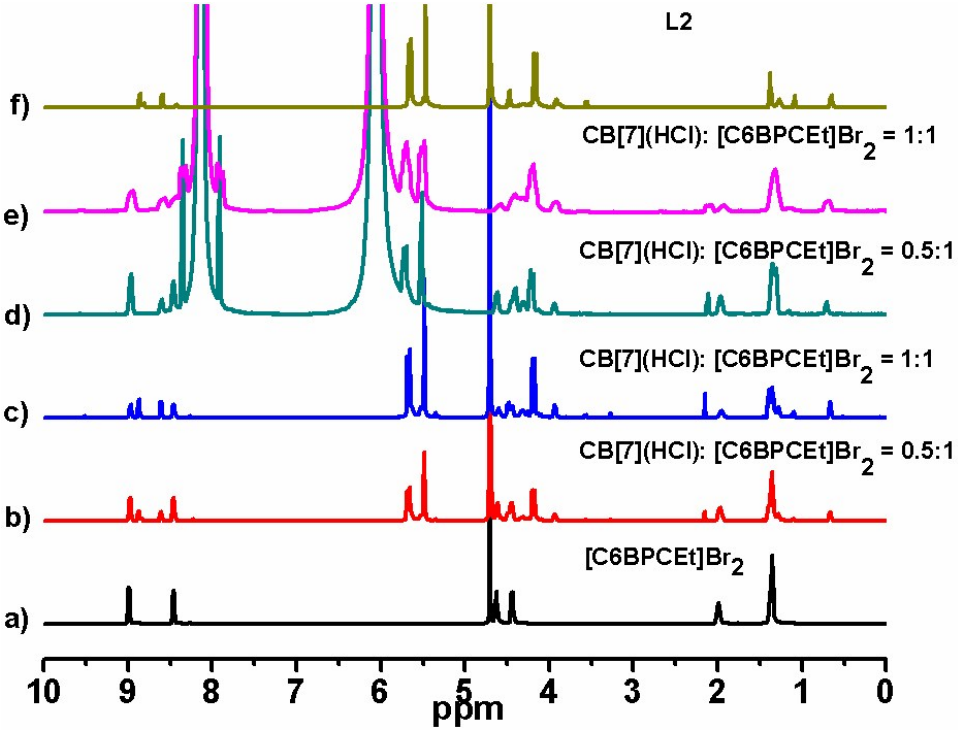

Figure S18. Binding experiments of $[C6BPCEt]Br_2$ with CB[7](HCl) in pure D_2O and in D_2O-HCOOH (1:1, v/v). Concentrations: a) $[C6BPCEt]Br_2$; b) CB[7](HCl) /$[C6BPCEt]Br_2$ = 0.0061/0.011 mol/L in pure D_2O; c) CB[7](HCl) /$[C6BPCEt]Br_2$ = 0.012/0.011 mol/L in pure D_2O; d) CB[7](HCl) /$[C6BPCEt]Br_2$ = 0.0055/0.0097 mol/L D_2O-HCOOH (1:1, v/v); e) CB[7](HCl) /$[C6BPCEt]Br_2$ = 0.0099/0.011 mol/L in D_2O-HCOOH (1:1, v/v); f) L2.

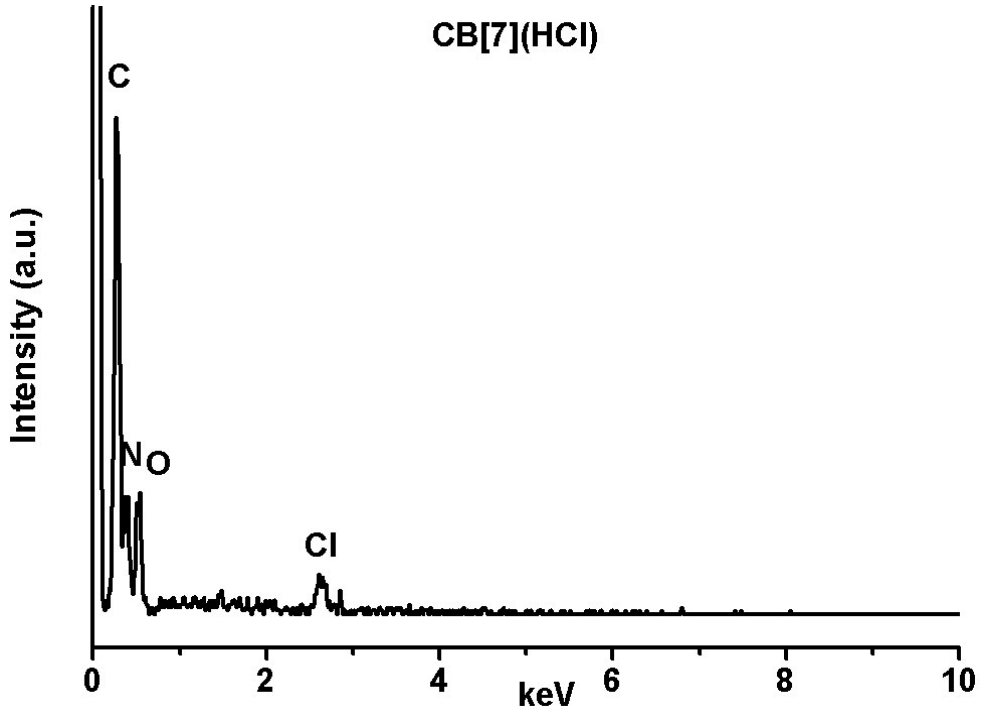

Figure S19. EDS spectrum of CB[7](HCl) revealing the typical peaks of C, N, O and Cl elements.

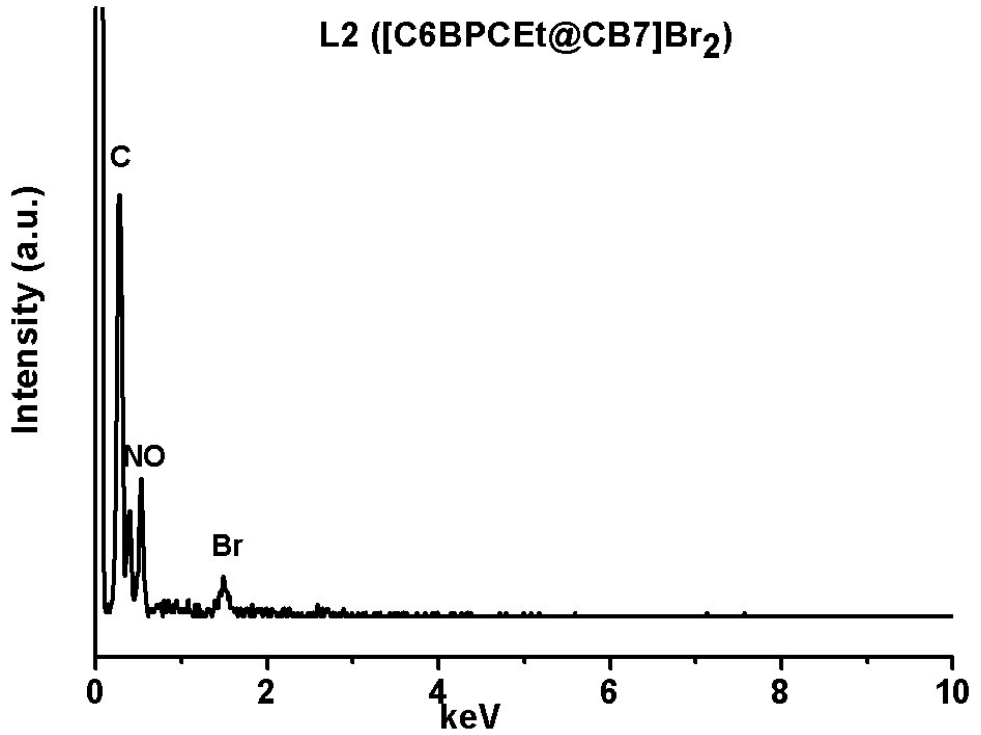

Figure S20. EDS spectrum of **L2** revealing the typical peaks of C, N, O and Br elements.

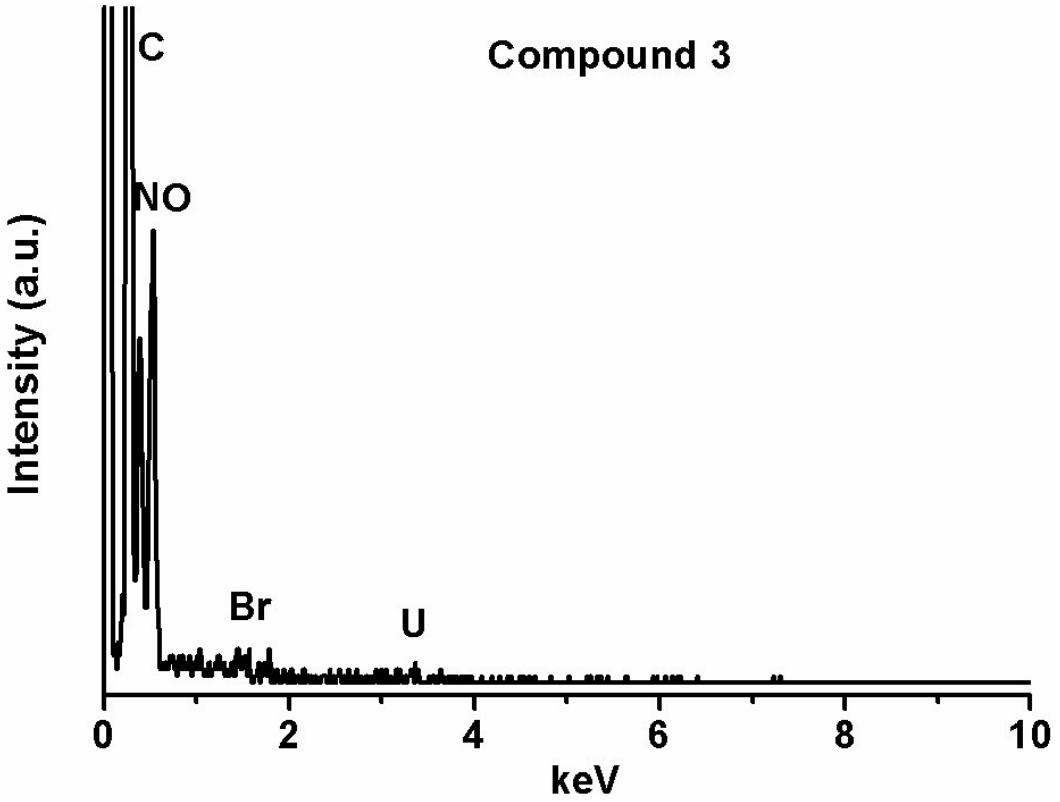

Figure S21. EDS spectrum of compound **3** revealing the typical peaks of C, N, O, Br and U elements.

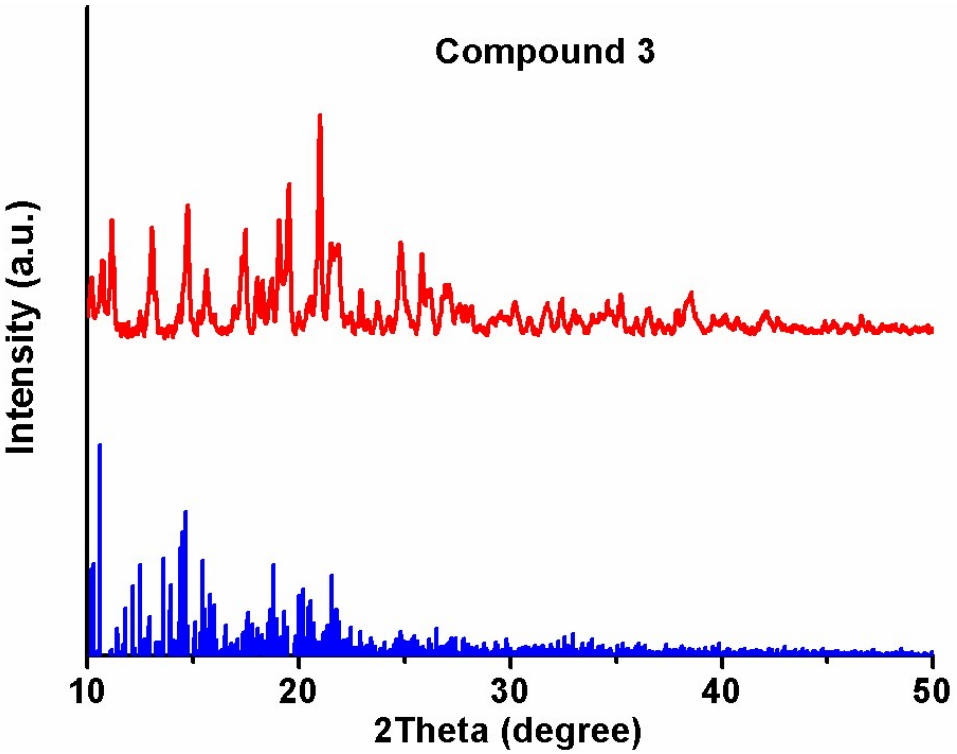

Figure S22. Powder X-Ray Diffraction of compound **3**. The upper and lower parts for each diagram are experimental spectra and simulated spectra from single crystal data.

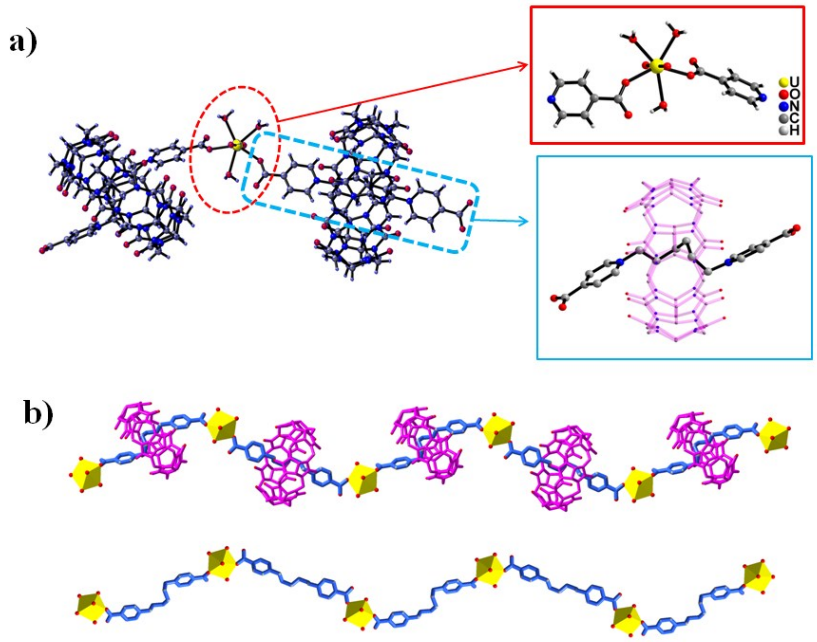

Figure S23. Structural building unit of compounds **3** containing a uranyl center in **s**even-fold coordination pentagonal biyramid geometry and rotaxane linkers with folded string chains.

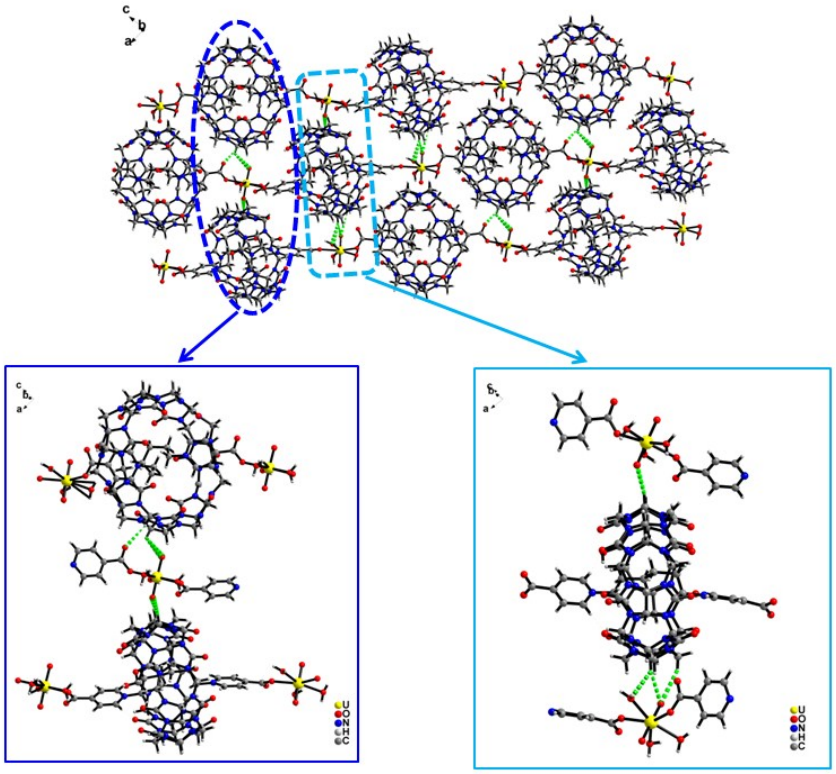

Figure S24. C-H•••O hydrogen bonding between cucurbituril macrocycles and uranyl motifs in adjacent chain contribute to the close packing of compound **3** (top): uranyl motifs interact with cucurbituril macrocycles in adjacent sheets from two different directions (left in the bottom) and cucurbituril macrocycles also interact with uranyl motifs in adjacent sheets from two different directions (right in the bottom).

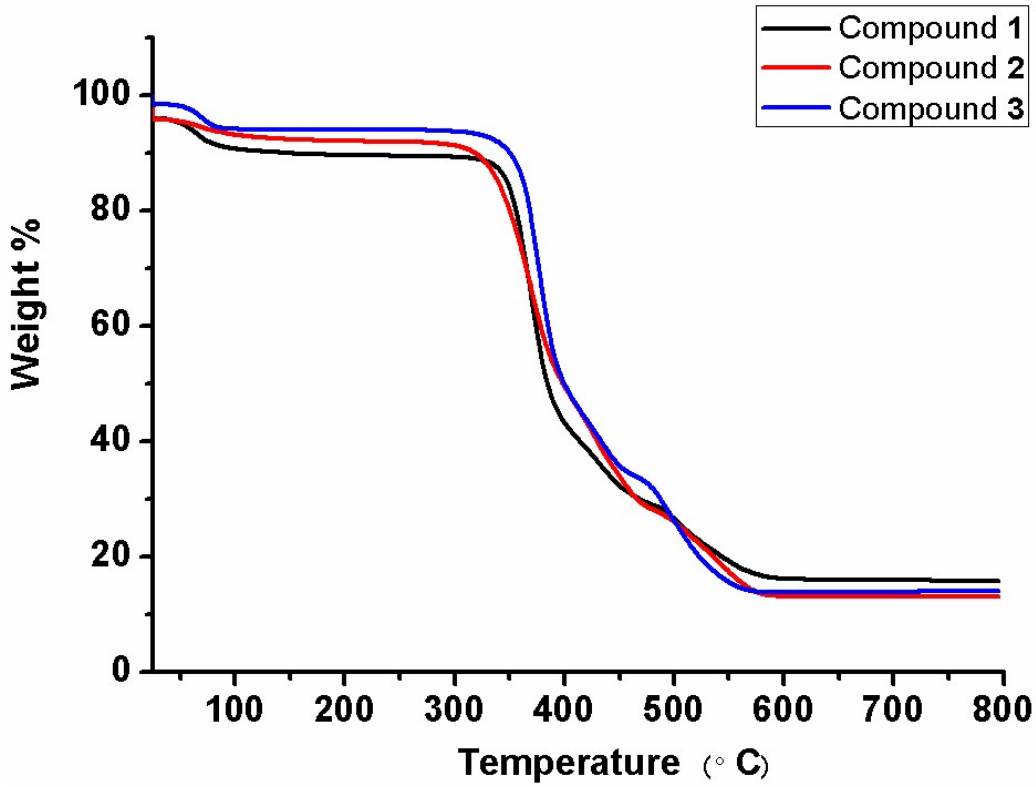

Figure S25. Thermogravimetric results for compounds **1**-**3**.

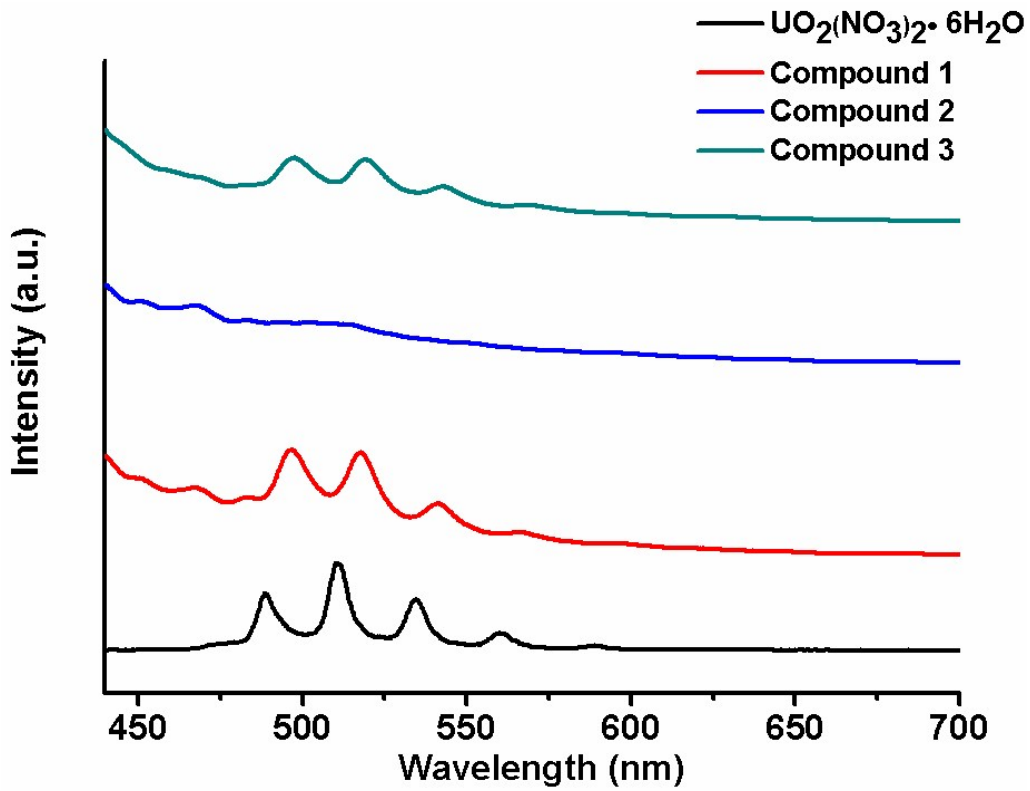

Figure S26. Thermogravimetric results for compounds **1**-**3** using uranyl nitrate as a control.

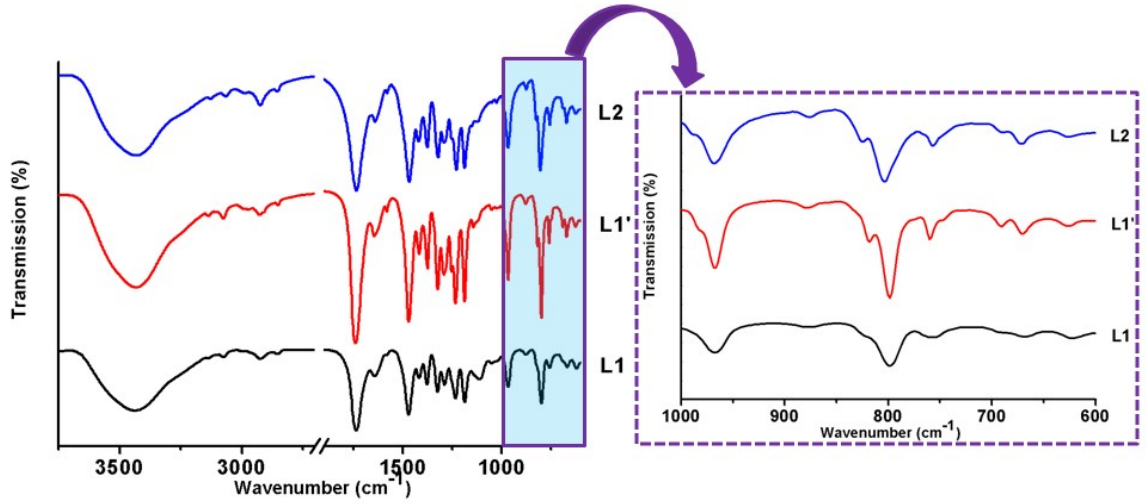

Figure S27. The IR spectra of precursor**s L1**, **L1'** and **L2**.

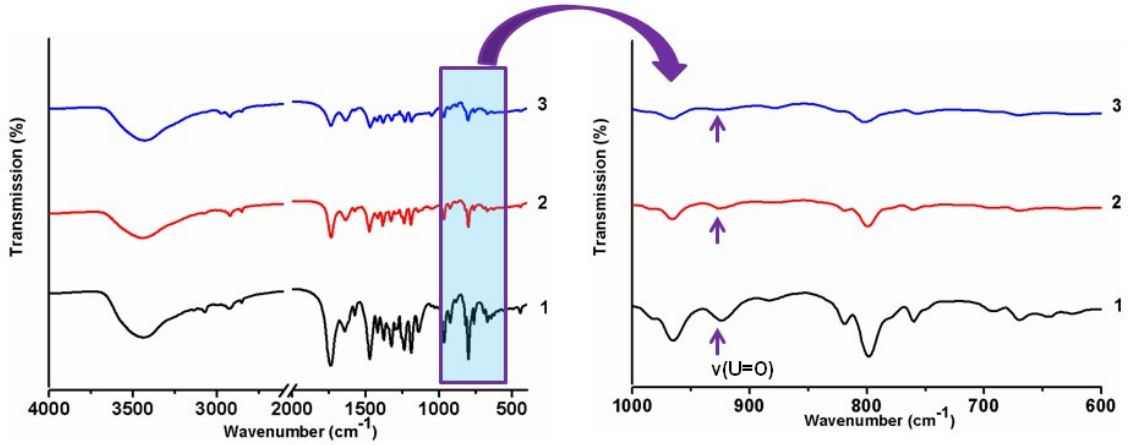

Figure S28. The IR spectra of uranyl compounds **1-3**, with [U=O] stretching band in the region of ~924 cm^{-1}.

S3. Typical Tables

Table S1. Crystal data and structure refinement for uranyl compounds **1-3**.

	1	**2**	**3**
formula	$C_{54}H_{56}N_{26}O_{22}SU$	$C_{108}H_{112}Br_2N_{52}O_{34}U$	$C_{120}H_{136}Br_2N_{60}O_{46}U_2$
formula weight	1691.34	3080.35	3790.77
crystal system	triclinic	triclinic	triclinic
space group	$P\bar{1}$	$P\bar{1}$	$P\bar{1}$
a, Å	15.4905(4)	12.6458(3)	13.333(3)
b, Å	15.7934(5)	15.6109(3)	26.409(5)
c, Å	16.7184(6)	17.1344(5)	26.515(5)
α, deg	68.423(3)	89.597(2)	81.73(3)
β, deg	89.602(3)	82.238(2)	84.73(3)
γ, deg	83.048(3)	84.826 (2)	84.24(3)
V, Å^3	3772.4(2)	3282.6(2)	9164(3)
Z	2	1	2
T, K	293	293	293
F(000)	1692.0	1558.0	3796.0
Dc, g/cm^3	1.489	1.532	1.374
μ **(mm^{-1})**	[a] 7.054	[a] 4.935	[b] 2.286
R_{int}	0.0318	0.0240	0.0770
R_1, wR_2 (all data)	0.0354, 0.0985	0.0484, 0.1329	0.0726, 0.1960

[a] μ (Cu Kα,). [b] μ (Mo Kα,).

Table S2. Selected bond distances (Å) related to uranyl centers and distances (Å) for hydrogen bonds observed in uranyl compounds **1-3**.

		1	
U(1)-O(1)	1.768(4)	C(26)-H(26A)···O(9)	2.465(5)
U(1)-O(2)	1.762(4)	C(23)-H(23)···O(9)	2.661(5)
U(1)-O(3)	2.348(3)	C(15)-H(15A)···O(20)	2.584(3)
U(1)-O(4)	2.365(5)	C(44)-H(44B)···O(21)	2.554(3)
U(1)-O(5)	2.311(4)	C(57)-H(57A)···O(21)	2.611(3)
U(1)-O(7)	2.443(5)	C(14)-H(14A)···O(22)	2.318(3)
U(1)-O(8)	2.432(4)	C(14)-H(14A)···O(22)	2.318(3)
C(11)-H(11B)···O(1)	2.443(4)	C(15)-H(15B)···O(22)	2.387 (4)
C(32)-H(32)···O(2)	2.393(3)	C(56)-H(56)···O(23)	2.036(4)
C(37)-H(37)···O(8)	2.399(4)	C(41)-H(41)···O(24)	2.435(4)
C(22)-H(22)···O(8)	2.667(6)		
		2	
U(1)-O(1)	1.757(4)	C(20)-H(20)···O(9)	2.314(3)
U(1)-O(2)	2.272(5)	C(53)-H(53)···O(10)	2.239(3)
U(1)-O(4)	2.647(8)	C(4)-H(4B)···O(11)	2.445(3)
U(1)-O(5)	2.679(7)	C(4)-H(4A)···O(13)	2.700(3)
U(1)-O(7)	2.243(9)	C(37)-H(37)···O(13)	2.259(4)
C(13)-H(13)···O(1)	2.410(4)	C(23)-H(23A)···O(14)	2.444(3)
C(9)-H(9)···O(1)	2.678(5)	C(31)-H(31)···O(15)	2.334(3)
C(9)-H(9)···O(3)	2.665(5)	C(23)-H(23B)···O(18)	2.404(4)
C(47)-H(47B)···O(3)	2.266(4)	C(23)-H(23A)···O(19)	2.614(3)
C(25)-H(25)···O(4)	2.499(7)	C(58)-H(58)···O(19)	2.251(4)
C(39)-H(39)···O(5)	2.681(7)	C(38)-H(38B)···Br(1)	2.832(5)
C(4)-H(4A)···O(9)	2.436(3)	C(52)-H(52)···Br(1)	2.740(5)
C(20)-H(20)···O(9)	2.314(3)		
		3	
U(1)-O(1)	1.770(4)	C(59)-H(59)···O(5)	2.629(5)
U(1)-O(2)	1.772(5)	C(51)-H(51B)···O(6)	2.653(6)
U(1)-O(3)	2.375(5)	C(37)-H(37)···O(9)	2.301(5)
U(1)-O(4)	2.345(6)	C(85)-H(85)···O(11)	2.433(5)
U(1)-O(5)	2.481(6)	C(27)-H(27A)···O(27)	2.776(5)
U(1)-O(6)	2.380(6)	C(71)-H(71)···O(29)	2.499(6)
U(1)-O(7)	2.453(5)	O(15)-H(15D)···O(31)	1.910(5)
U(2)-O(10)	1.775(5)	C(39)-H(39A)···O(31)	2.387(5)
U(2)-O(11)	1.779(5)	O(6)-H(6B)···O(32)	2.009(5)
U(2)-O(12)	2.373(8)	C(92)-H(92)···O(32)	2.740(5)
U(2)-O(13)	2.363(5)	C(97)-H(97)···O(34)	2.388(5)
U(2)-O(14)	2.491(5)	C(107)-H(127)···O(40)	2.501(6)
U(2)-O(15)	2.419(5)	C(27)-H(27B)···O(46)	2.469(5)
U(2)-O(16)	2.382(6)	C(46)-H(46A)···O(51)	2.596(5)
C(20)-H(20B)···O(1)	2.657(4)	C(106)-H(106)···O(61)	2.445(5)
C(26)-H(26)···O(1)	2.413(5)	C(32)-H(32)···O(76)	2.560(7)
C(59)-H(59)···O(1)	2.592(5)		